JOURNAL OF MATERIALS SCIENCE 16 (1981) 3067–3076

Phase equilibria and ordering in the erbia-zirconia system

C. PASCUAL,* P. DURAN
C.S.I.C. Instituto de Cerámica y Vidrio, Departamento de Materiales, Cerámicos Especiales, Arganda del Rey, Madrid, Spain

The phase diagram for the system ZrO_2–Er_2O_3 was redetermined. At high temperatures, the system is dominated by wide regions of solid solution based on ZrO_2 and Er_2O_3 separated by a two-phase field which appears to extend to the solidus. The range of existence of these solid solution fields was determined using the precision lattice parameter method. A low-temperature (< 1800° C) long-range ordering occurred between 20 and 90 mol % Er_2O_3, and three ordered phases were found: the first compound was present at 40 mol % Er_2O_3 and corresponds to the ideal formula $Er_4Zr_3O_{12}$ with rhombohedral symmetry (space group $R\bar{3}$), is isostructural with UY_6O_{12}, and decomposes at about 1500° C into fluorite solid solution by an order–disorder process; the second ordered phase is formed at about 55 mol % Er_2O_3, its formula is close to $Er_5Zr_2O_{11.5}$, and it decomposes at about 1650° C into cubic solid solutions of the fluorite and C-type; the third compound is formed at 75 mol % Er_2O_3, its formula is Er_6ZrO_{11}, it has a wide homogeneity range, and it decomposes above 1700° C into a cubic solid solution of the C-type. Liquidus determination indicated the existence of a peritectic at 62 mol % Er_2O_3.

1. Introduction

The first detailed study of the zirconia–erbia system was that of Rouanet [1]. He determined the high-temperature (> 1800° C) phase relations and the liquidus curve for this system; the fluorite structure was found for 10 mol % Er_2O_3, and the system was dominated by two wide regions of solid solution based on fluorite and C-type structures with a continuous transition between them. The transition temperature for cubic erbia to hexagonal Er_2O_3 was also reported. Stewart *et al.* [2] studied the stabilization of ZrO_2 by Er_2O_3 and found that a two-phase field, consisting of monoclinic and tetragonal zirconia solid solutions, exists up to 4.45 mol % Er_2O_3, at which concentration the major phase was tetragonal. At higher erbia contents the fluorite solid solution was present as the only phase. No ordered phases were observed.

More recently, Thornber *et al.* [3] studied the fluorite-related phases in the ZrO_2–Ln_2O_3 (Sc, Yb, Er, Dy) systems, and ordered phases of the M_7O_{12}-type (40 mol % Er_2O_3) were reported. This phase, and its crystal structure, was also confirmed by Rossell [4]. A previous paper [5] reported no definitive data on this system mainly in that related to the extent of the ordered phases and the fluorite–C-type solid solutions transition at high temperature.

The present work describes experiments on erbia–zirconia mixtures using both samples sintered up to 2000° C, for the tetragonal–monoclinic zirconia transformation and ordering phenomena studies, and melted samples quenched from high temperature to retain equilibrium.

2. Experimental technique

The general details of sample preparation, heating, thermal expansion measurements, and X-ray diffraction pattern (at room and high temperature) analysis have been described elsewhere [5].

In the zirconia-rich region, the compositions

*This work is based on the Ph.D. thesis of C. Pascual, Madrid University, 1980.

0022–2461/81/113067–10$03.00/0

studied ranged from 0 to 10 mol% Er_2O_3 in steps of 0.5 mol% for the determination of the martensitic monoclinic–tetragonal transformation in zirconia, by using differential thermal analysis (DTA), and with Al_2O_3 as reference material. Taking into account the effect of heating rate on the monoclinic–tetragonal zirconia transformation, a heating rate of 8° C min^{-1} was found to be the most suitable for determining the transformation. The relative magnitude of the heat effect was expressed in microvolts, taking into account the intensity of the DTA peak for each sample and that of the zirconia pure. To minimize the crystallite size-effect on the relative values reported here, the samples were prepared in an identical manner in all cases.

For the high-temperature experiments, the compositions studied ranged from 50 to 90 mol% Er_2O_3. Heating at 1800° C and above was carried out on Mo strips in a 5 vol% H_2–95 vol% Ar mixture. The temperature was measured with an optical pyrometer calibrated at the melting point of Al_2O_3 and the precision of temperature measurements was no better than ± 40° C. The heating time was 2 h in all the cases. Compositions ranging from 50 to 70 mol% Er_2O_3 were melted in a solar furnace and then slowly solidified unidirectionally to study the composition of the separated phases at high temperature.

At low temperatures (< 1800° C) experiments at 1760, 1550, 1400, 1150 and 800° C were performed with sintered and melted samples. At each temperature the samples were held for long enough to establish equilibrium and then quenched rapidly in air before being examined by X-ray diffraction pattern analysis. To study the low-temperature ordering, a series of experiments was carried out at temperatures from 800 to 1150° C with prolonged heating for up to as much as 8 months on compositions ranging from 20 to 90 mol% Er_2O_3.

The phases present in the quenched samples were identified by X-ray diffraction pattern analysis and the phase boundaries of the cubic field were determined from precision lattice parameter measurements. The scan rate was 0.25° min^{-1}. Ni-filtered Cu radiation was used, and only the diffraction lines with diffraction angles $2\theta > 60°$ were used for the lattice parameter determinations. A lattice parameter was calculated from each line and these data were plotted as a function of $\frac{1}{2}(\cos^2\theta/\sin\theta + \cos^2\theta/\theta)$ to obtain the corrected value of the lattice parameter, a_0. The extrapolated values of a_0 were obtained by a least-square fit analysis of the data.

To determine the defect model in the fluorite solid solutions the apparent densities were considered. The apparent densities were measured by a liquid displacement method, using tetrachloroethylene (of density 1.6224 g cm^{-3}) as the liquid, for specimens of various Er_2O_3 concentrations sintered at about 2000° C and annealed in air at 1550° C for several h.

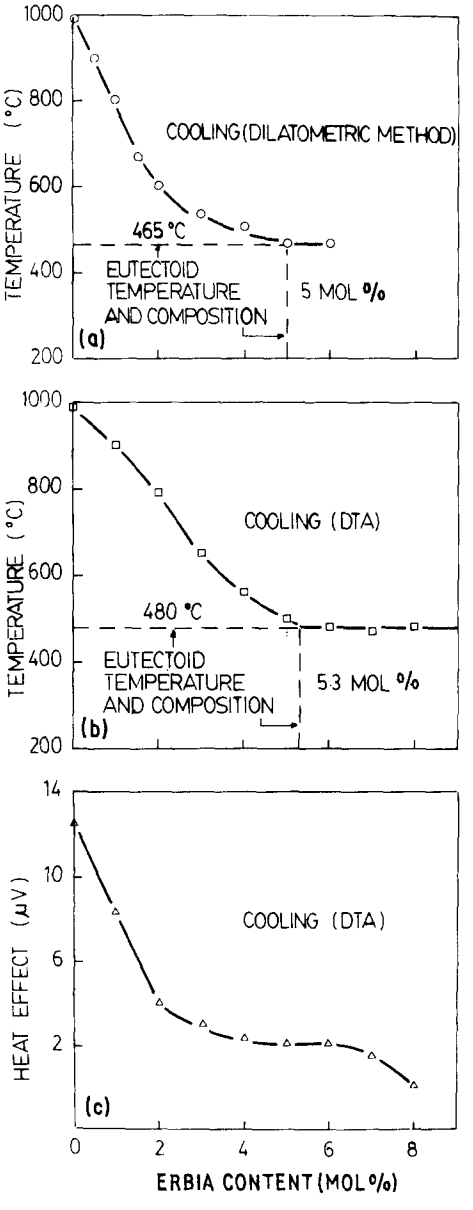

Figure 1 The tetragonal–monoclinic transformation and heat effect against Er_2O_3 content in the ZrO_2–Er_2O_3 system.

3. Results

3.1. The tetragonal–monoclinic zirconia transformation

The results of thermal expansion measurements and DTA are summarized in Fig. 1. The influence of Er_2O_3 additions on the temperature of the zirconia transformation, measured by the dilatometric method, is shown in Fig. 1a. As may be seen, the transformation temperature decreases steadily up to ~ 5 mol% Er_2O_3 and then remains constant at 461° C. Fig. 1b shows a plot of the tetragonal–monoclinic transformation temperature of zirconia plotted against composition, investigated by DTA. As Er_2O_3 is added to ZrO_2, the transformation temperature decreases sharply up to 3 mol% Er_2O_3. Beyond this concentration the transformation temperature decrease procedes more slowly up to 5.3 mol% Er_2O_3 at 480° C and then remains constant. Fig. 1c shows the heat effect observed in the transformation plotted against Er_2O_3 content. This heat effect decreases rapidly up to ~ 2 mol% Er_2O_3; beyond this concentration the effect decreases slowly and at 8 mol% Er_2O_3 it disappears. This result agrees with that of Ruh *et al.* [6], for the ZrO_2–Sc_2O_3 and ZrO_2–Y_2O_3 systems, who found that the height of the DTA peaks decrease continuously with increasing Sc_2O_3 or Y_2O_3 contents, and reach a value of zero at 4 and 2.5 mol%, respectively. However, our results are in disagreement with those of Srivastava *et al.* [7] who found in the ZrO_2–Y_2O_3 system that the heat effect (cal g^{-1}) increases up to 1 mol% Y_2O_3, and then decreases with the Y_2O_3 content.

From Fig. 1a, b and c it is clearly seen that as the Er_2O_3 content increases up to ~ 2 mol%, the tetragonal–monoclinic transformation temperature and the heat effect both decrease sharply. This concentration can be considered as being the limit of the monoclinic zirconia solid solution, which is in close agreement with the observations of Stewart *et al.* [2] (2.22 mol% Er_2O_3). At higher Er_2O_3 concentrations, the transformation temperature and the magnitude of the heat effect decrease slowly with decreasing amounts of monoclinic-phase present in the sample. For compositions ranging between 5 and 7 mol% Er_2O_3, the temperature for the tetragonal–monoclinic transformation remains constant. These results, and the variation of the amounts of the coexisting phases of these samples with temperature, determined by high-temperature X-ray diffraction pattern analysis, show that a eutectoid reaction between monoclinic and cubic zirconia occurs in the vicinity of 5 mol% Er_2O_3 at about 470° C.

3.2. High-temperature solid solutions and the transition fluorite–C-type structures

Above 1600° C, the compositions containing from 10 to 50 mol% Er_2O_3 were single-phase with the fluorite structure. The lower limits of the fluorite solid solution has been defined quite accurately at 1600, 1720 and 2000° C, by determining the lattice parameters of the cubic phase, and were found to be 4.5, 4 and 2 mol% Er_2O_3, respectively.

As Er_2O_3 is added to zirconia, the lattice parameter of the composition ranging between 10 and 40 mol% Er_2O_3 varied linearly with concentration of erbia, indicating that Er_2O_3 can form a solid solution with ZrO_2 in this range.

In order to preserve electrical neutrality in the solid solution, chemical defects are necessary, and the charge neutrality can be maintained by one of the two following structural defect models:

(a) all metal ions remain fixed at the lattice points and the appropriate number of anion vacancies are created; and

(b) all oxygen ions remain fixed and the excess cations occupy interstitial sites.

The only difference between the two structural defect models is the addition of extra cations or the absence of oxygen ions within a unit volume and this should lead to differing densities for the two models; by comparing the calculated densities with the measured apparent densities, the defect model can be determined. Fig. 2 shows the calcu-

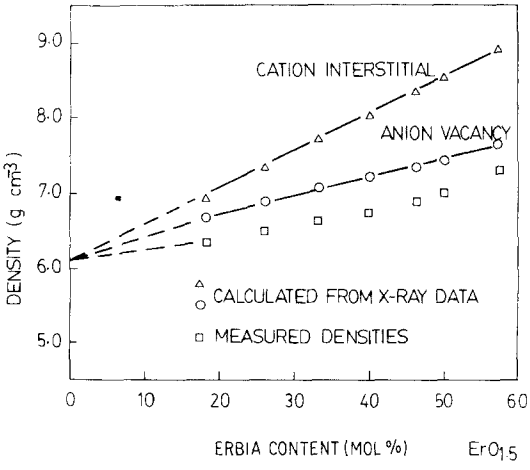

Figure 2 Calculated and measured densities of the ZrO_2–Er_2O_3 system as a function of Er_2O_3 content.

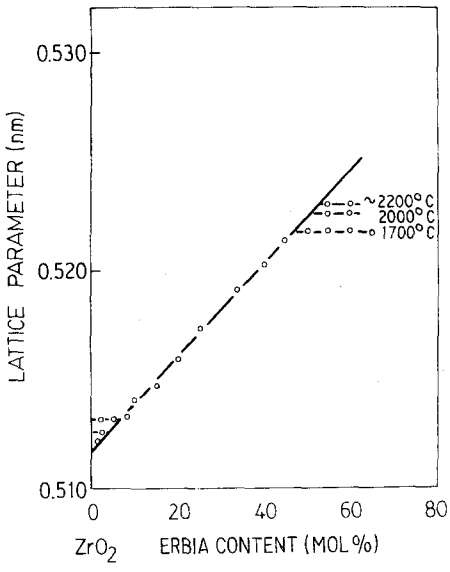

Figure 3 Lattice parameters of cubic ZrO_2 solid solution plotted against Er_2O_3 content for various temperatures.

lated and measured densities of the ZrO_2–$ErO_{1.5}$ system as a function of $ErO_{1.5}$ content. The present results show that the calculated values based on the structural defect model (a) are in close agreement with the measured values, and it has been concluded that the cubic solid solutions (10 to 40 mol% Er_2O_3) in the ZrO_2–Er_2O_3 system have an imperfect fluorite lattice containing vacant oxygen sites. Similar results were also obtained for the ZrO_2–CaO [8], ZrO_2–Y_2O_3 [9] and HfO_2–Y_2O_3 [10] systems.

The solubility limits of Er_2O_3 in ZrO_2 at the right of the fluorite domain are established to be 40 mol% Er_2O_3 at 1700° C, 51 mol% Er_2O_3 at 2000° C and 53 mol% Er_2O_3 at about 2200° C. Beyond these limits, a two-phase field [fluorite- and C-type solid solutions ($F_{ss} + C_{ss}$)] exists. Between 55 and 70 mol% Er_2O_3, the samples quenched from above the liquidus temperature segregated during the cooling, but the parameters of the fluorite- and C-type phases varied with the overall sample composition, which indicates that the equilibrium is very difficult to retain on quenching. However, when these samples were annealed at 2000° C the miscibility gap was clearly established. Annealing at 2000° C has the effect of improving the crystallinity and making more readily detectable the two-phase field present at higher temperatures. Figs 3 and 4 show the relation between lattice parameters and composition for the fluorite- and C-type solid solutions.

The lattice parameter a (in nm) for the fluorite- or C-type cell, can be expressed as

$$a = 0.5117 + 0.00021\,x, \text{ for } 10 \leqslant x \leqslant 40$$

or

$$a = 1.0423 + 0.00012\,x, \text{ for } 65 \leqslant x \leqslant 95,$$

where x is the erbia content (mol%).

The cubic erbia solid-solution field extends from pure erbia to 37 mol% ZrO_2 at ~ 2200° C, and to 35 mol% ZrO_2 at 1800° C.

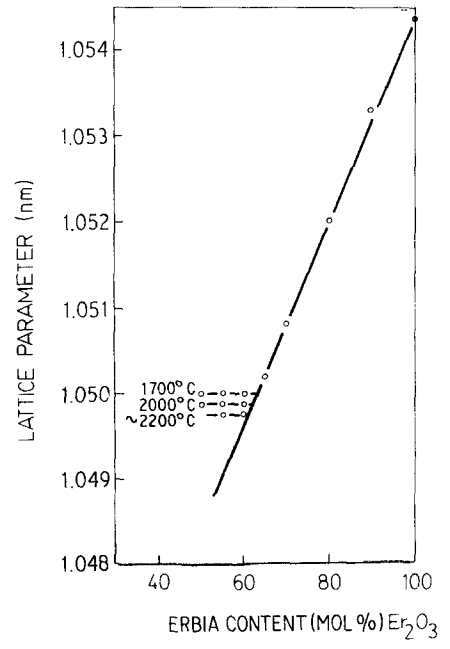

Figure 4 Lattice parameters of cubic Er_2O_3 solid solution plotted against Er_2O_3 content for various temperatures.

3.3. Ordering phenomena at low temperature

In order to establish with precision the composition and extent of the ordered phases present in this system, sintered and melted samples in the concentration range 20 to 90 mol% Er_2O_3 were heat-treated between 700 and 1800° C. The samples were annealed for several months at 1150° C with grinding and pelletizing at monthly intervals. After 4 to 6 months at 1150° C, the samples containing less than 30 mol% Er_2O_3 are single-phase with fluorite-type structure: it was necessary to extend the heat-treatments to 8 months in order to detect any ordering in the sintered and melted samples.

Sintered samples containing > 30 mol% Er_2O_3,

annealed for two or more months at 1150° C, presented the following phase sequence: fluorite solid-solution + $Er_4Zr_3O_{12}$ for the 30, 33.3 and 35 mol% Er_2O_3 compositions. The δ-phase ($Er_4Zr_3O_{12}$) was clearly detected in the 40 mol% Er_2O_3 composition. Between 40 and 55 mol% Er_2O_3 two hexagonal phases were found, one with composition $Er_4Zr_3O_{12}$ and the other with composition $Er_5Zr_2O_{11.5}$. The second hexagonal phase $Er_5Zr_2O_{11.5}$ was present as the only phase in the 55 mol% Er_2O_3 composition. A new mixture of two hexagonal phases was present between 55 and about 63 mol% Er_2O_3, corresponding to $Er_5Zr_2O_{11.5}$ (55 mol% Er_2O_3) and Er_6ZrO_{11} (75 mol% Er_2O_3), respectively. The third hexagonal phase, Er_6ZrO_{11}, shows a wide homogeneity range which extends from about 63 to 90 mol% Er_2O_3.

In order to investigate the formation and stability of the three hexagonal phases, sintered and melted samples containing 40, 45, 55, 57 and 75 mol% Er_2O_3 were annealed for several periods of time between 800 and 1800° C. For the sample with 40 mol% Er_2O_3 composition, after one month at 1150° C, no sign of ordering was observed for the sintered and melted samples. It was necessary to prolong the heat-treatment by up to two months to detect any ordering in the sintered sample and no ordering was detected in the melted sample. In the sintered sample the ordered phase $Er_4Zr_3O_{12}$ was only obtained clearly after heat-treatment for three or more months at 1150° C. In the case of the melted sample, ordering was detected only after heat-treatment for 6 to 8 months at 1150° C.

This ordered phase can be indexed on the basis of a hexagonal unit cell, but the true symmetry of the phase is rhombohedral since only $-h + k + l = 3n$ reflections are present. Fig. 5 shows the X-ray powder diagram and Table I shows the indexing for the $Er_4Zr_3O_{12}$ phase. $Er_4Zr_3O_{12}$ is isostructural with UY_6O_{12} and shows a ratio a_H/c_H (where the subscript H indicates the hexagonal phase) that is close to the ideal value of 1.0801. Its general formula is M_7O_{12}, and has a structure that involves an anion-deficient rhombohedral distortion of the fluorite lattice. The space group is $R\bar{3}$ with one of the (1 1 1) cubic directions becoming the unique three-fold inversion axis of the rhombohedral cell. The oxygen vacancies are aligned along the (1 1 1) directions, thereby resulting in infinite chains of six-co-ordinated metal cations following the three-fold axis [11].

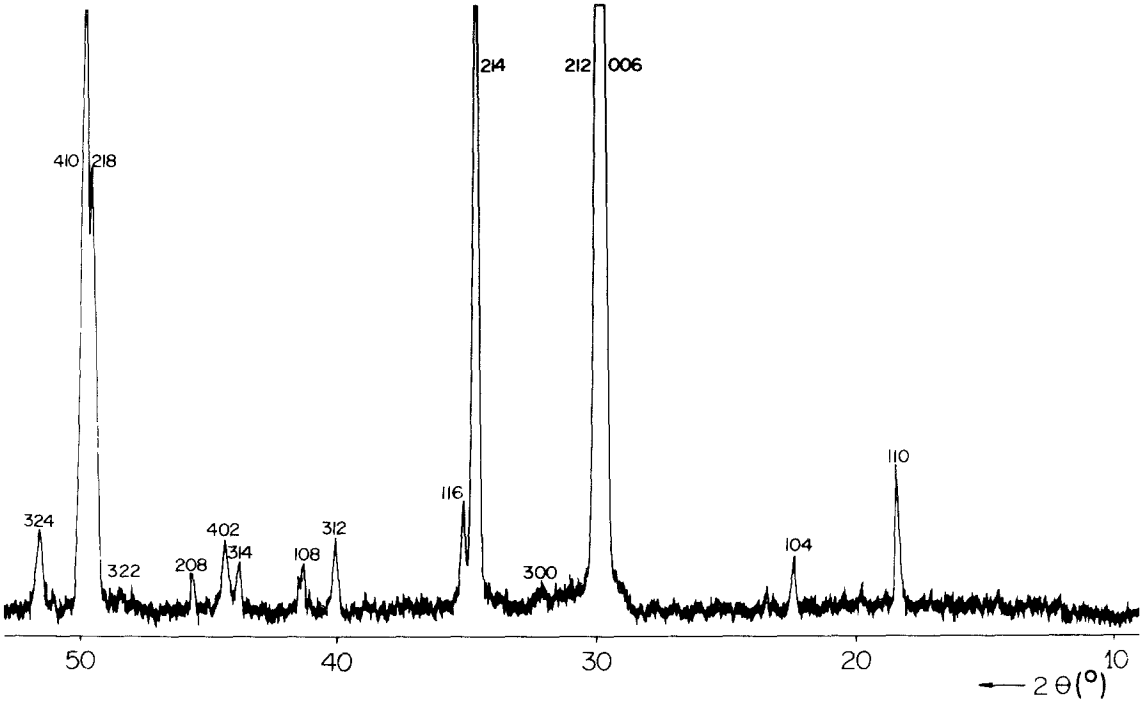

Figure 5 X-ray diffraction pattern of ZrO_2–Er_2O_3 (40 mol% Er_2O_3) composition treated at 1150° C for 4 months.

TABLE I Characteristic lines observed for $Er_4Zr_3O_{12}$ (hexagonal unit cell with $a = 0.9696 \pm 0.0003$ nm and $c = 1.8099 \pm 0.0006$ nm)

d spacing (nm)	Normalized line intensities (I/I_0)	$h\ k\ l$
0.483	3	1 1 0
0.396	15	1 0 4
0.301	39	0 0 6
0.299	100	2 1 2
0.279	1	3 0 0
0.259	28	2 1 3
0.259	3	1 1 6
0.225	2	3 1 2
0.218	2	1 0 8
0.206	2	3 1 4
0.204	3	4 0 2
0.198	15	2 0 8
0.189	1	3 2 2
0.184	25	2 1 8
0.183	39	4 1 0
0.177	3	3 2 4
0.162	25	3 1 8
0.158	5	2 1 10
0.157	7	4 1 6
0.156	31	4 2 2
0.153	15	4 0 8
0.150	3	0 0 12
0.149	6	4 2 4

In order to define the transition temperature to a disordered fluorite-type structure, small samples of the compound $Er_4Zr_3O_{12}$ were heated to increasing temperatures; in this way the transition to a disordered state was located at about 1500° C. It should be mentioned that at 1500° C the disordering of the $Er_4Zr_3O_{12}$ is sluggish and it therefore seems reasonable to assume that the value found for the transition temperature may not be very precise. The composition containing 45 mol% Er_2O_3, also heated at 1500° C, was single phase and of the fluorite-type; below 1500° C the composition was a mixture of the hexagonal phases $Er_4Zr_3O_{12}$ and $Er_5Zr_2O_{11.5}$. This result supports the contention that for this composition a eutectoid reaction takes place in the vicinity of 1450° C.

Samples containing 55 or 57 mol% Er_2O_3 showed the existence of the second hexagonal phase, and, as observed for the HfO_2–Er_2O_3 system [12], this phase has also been indexed to the composition $Er_5Zr_2O_{11.5}$, the unit cell contained six molecules ($M_{42}O_{69} = 30\,Er^{3+}$, $12\,Zr^{4+}$, $69\,O^{2-}$, $15\,\square$ [13], where $\square$ indicates a vacancy) and is isostructural with the hexagonal phase H_2 found in the ZrO_2–L_2O_3 (L = Gd, Dy, Yb) systems [14]. Since the lattice parameters measured on compositions on both sides of the ideal $M_7O_{11.5}$ composition remained constant, it was assumed that this compound is a line in the system. Its stability extends up to 1650° C and above this temperature decomposition takes place, producing two phases of the fluorite- and C-type structures.

Samples containing more than 65 mol% Er_2O_3 showed the existence of the third hexagonal phase of the M_7O_{11}-type. This phase is isostructural with the hexagonal phase H_3 previously found in the ZrO_2–Gd_2O_3, ZrO_2–Dy_2O_3 and ZrO_2–Yb_2O_3 systems [14], and for the HfO_2–Er_2O_3 system [12, 15]. This hexagonal phase represents a compound with the composition Er_6ZrO_{11} (close to 75 mol% Er_2O_3), with a unit cell containing also six molecules of compound [13], a region of homogeneity extending from approximately 65 to 90 mol% Er_2O_3, and a temperature range of existence between approximately 700 and 1800° C; above this temperature the compound transforms into solid solution of the C-type by order–disorder transition. Fig. 6 shows the X-ray powder diffractogram for the $Er_5Zr_2O_{11.5}$ and Er_6ZrO_{11} compounds.

The existence of two hexagonal phases ($Er_5Zr_2O_{11.5}$ and Er_6ZrO_{11}) at low temperature for the 60 mol% Er_2O_3 composition, leads to the assumption that another eutectoid reaction (C-type solid solution → $Er_5Zr_2O_{11.5}$ plus Er_6ZrO_{11} solid solution) takes place in this vicinity.

The ordered phases of the M_7O_{11}-type are related to the distorted fluorite cell, and the hexagonal unit cell of these compounds may be derived by applying the transformation matrix determined from the fluorite cell to the hexagonal subcell. In this sense, since the indices of the cubic line (1 1 1), after transition to a hexagonal subcell, are transformed into lines with indices (0 0 3) and (1 0 1), and since the interpretation of the powder diffraction pattern leads to indices (0 0 6) and (2 1 2), then, taking into account this change of the indices and the schematic situation presented in Fig. 7 for the reciprocal lattice of a particular domain, we have calculated the corresponding transformation of the axes to be $a_H = a_0\sqrt{7}$ and $c_H = 2c_0$. Table II shows the phases found and their parameters on samples annealed for 6 to 8 months at 1150° C in the concentration range 20 to 90 mol% Er_2O_3.

Samples containing more than 90 mol% Er_2O_3 were a single phase of the C-type.

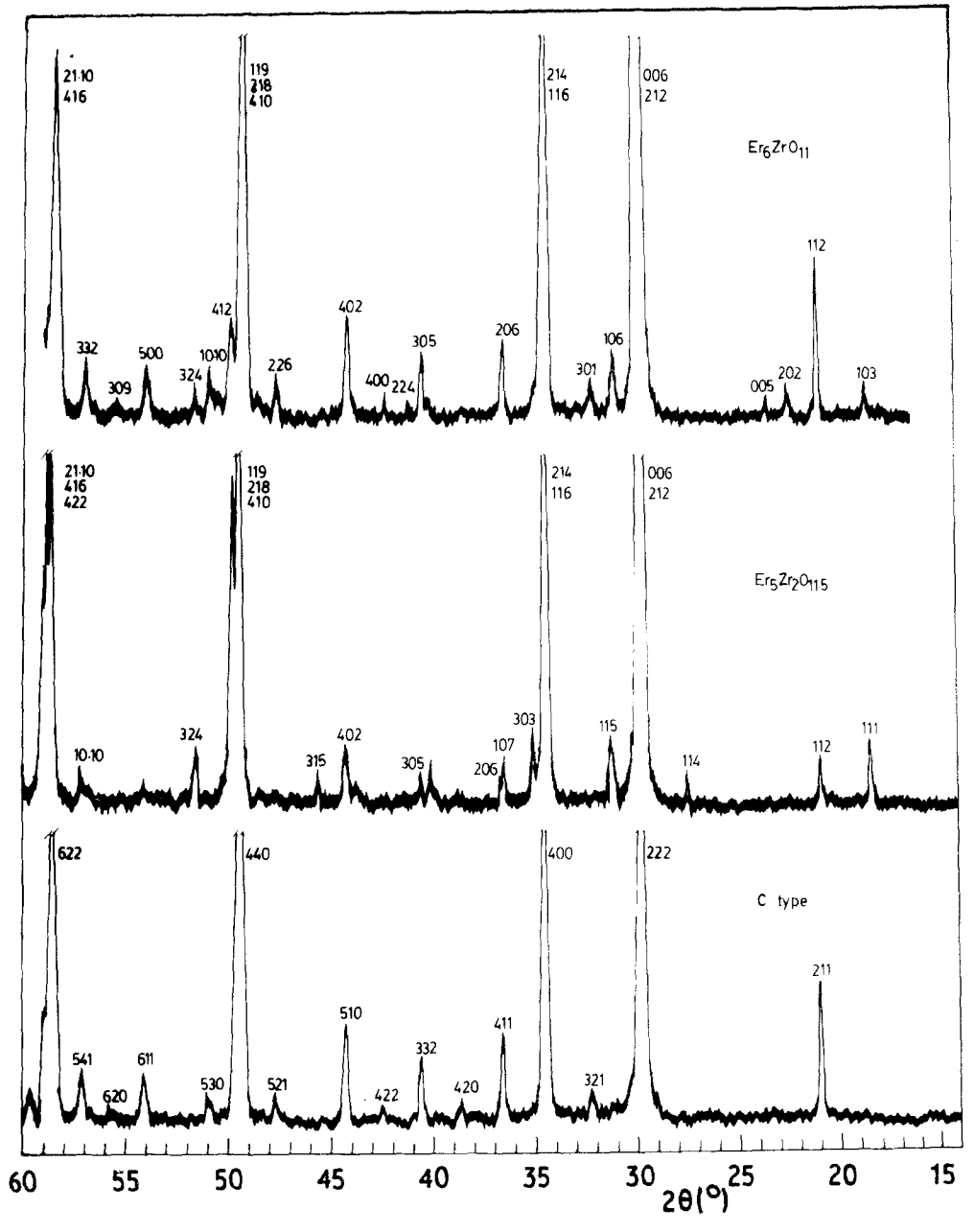

Figure 6 X-ray diffraction pattern of ZrO_2–Er_2O_3 (55 and 75 mol% Er_2O_3) compositions quenched from 1450° C.

3.4. The liquidus

Previous studies by Rouanet [1] on the ZrO_2–Er_2O_3 system show a eutectic point at approximately 20 mol% ZrO_2 which is associated with a phase change from C-type to H (hexagonal)-type in pure erbia at high temperature. If this is so, then the diagram by Rouanet for the liquidus implies a continuous transition from fluorite- to C-type. However, in the present work it has been found that the solubility of ZrO_2 in Er_2O_3 increases with increasing temperature up to the solidus. On the other hand, the composition containing 60 mol% Er_2O_3 provides no evidence for the existence of the hexagonal-type erbia in the melting vicinity. These results lead, therefore, to the assumption that a peritectic region may exist in the system at about 62 mol% Er_2O_3 which is incorporated in the solidus.

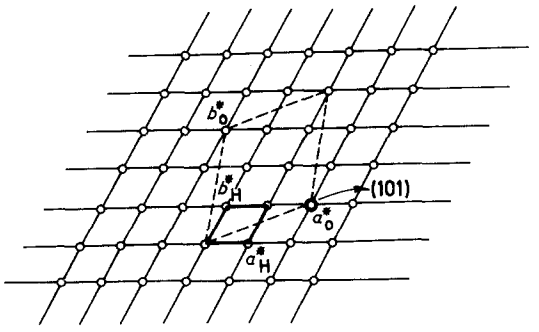

Figure 7 The reciprocal lattice of Er_6ZrO_{11} for a particular domain.

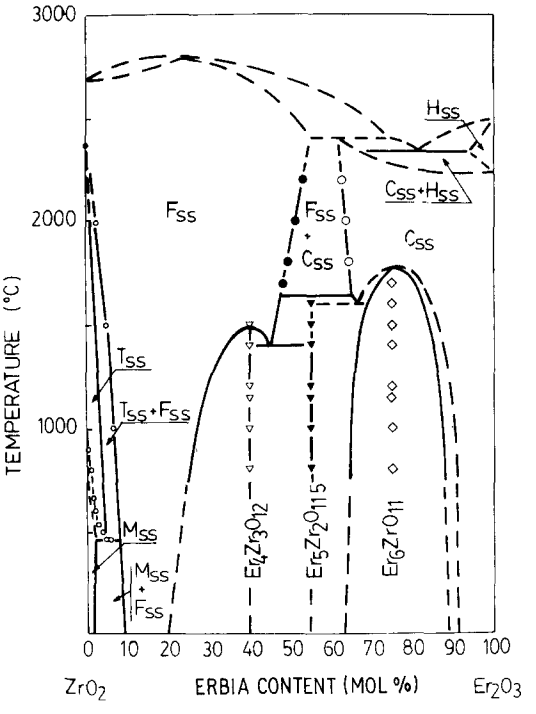

Figure 8 Tentative phase diagram for the ZrO_2–Er_2O_3 system.

4. Discussion

Based on the present data, the more important features from this work, illustrated in Fig. 8, are the discontinuous transition between the fluorite- and C-type rare-earth oxide structures at high temperature and, therefore, the proposed existence of a peritectic region in the phase diagram. At low temperature, a long-range ordering exists between 20 and 90 mol% Er_2O_3, and three ordered phases were found. These features differ markedly from those of previous studies [5] and also from those on the similar HfO_2–Er_2O_3 system [15, 16].

Another important feature is that the solubility of zirconia in erbia increases with increasing temperature, from about 35 mol% ZrO_2 at 1700° C to 38 mol% ZrO_2 at approximately 2200° C. This result is in close agreement with both a previous work on this system [5] and the

TABLE II Phases present at 1150° C for the ZrO_2–Er_2O_3 system

Compositions (mol% Er_2O_3)	Phases present	Lattice parameters (nm)
2 0	F_{ss} + $Er_4Zr_3O_{12}$ ↑	$a = 0.5159$
2 5	F_{ss} + $Er_4Zr_3O_{12}$ ↑	
3 0	F_{ss} ↓ + $Er_4Zr_3O_{12}$ ↑	
3 3.3	F_{ss} ↓ + $Er_4Zr_3O_{12}$ ↑	
3 5	F_{ss} ↓ + $Er_4Zr_3O_{12}$ ↑	
4 0	$Er_4Zr_3O_{12}$	$a = 0.9696$ $c = 0.9049$
4 5	$Er_4Zr_3O_{12}$ + $Er_5Zr_2O_{11.5}$	
5 0	$Er_4Zr_3O_{12}$ + $Er_5Zr_2O_{11.5}$	
5 5	$Er_5Zr_2O_{11.5}$	$a = 0.9776$ $c = 0.9105$
6 0	$Er_5Zr_2O_{11.5}$ + Er_6ZrO_{11} ss	
6 5	Er_6ZrO_{11} ss	
7 0	Er_6ZrO_{11} ss	$a = 0.9807$ $c = 0.9234$
7 5	Er_6ZrO_{11}	$a = 0.9857$ $c = 0.9273$
8 0	Er_6ZrO_{11} ss	
8 5	Er_6ZrO_{11} ss	
9 0	C_{ss}	$a = 1.0533$

works of Spiridinov *et al.* [15] and Wilder *et al.* [16] on the similar HfO_2–Er_2O_3 system. The major discrepancy occurs at very high temperature where the two-phase field (fluorite- plus C-type solid solutions) has been considered as a domed region. This form was adopted on the basis of the liquidus line drawn using the data of Rouanet [1]. This view is inconsistent with the results of the experiments described here. Therefore, the phase boundaries above 2200° C are drawn in accordance with the phase rule, and the solidus curve is modified in order to incorporate the peritectic region which might exist in the system. Although such discontinuous transition between fluorite- and C-type structures was not determined with precision, the absence of hexagonal-type erbia at 60 mol% Er_2O_3 in both the melted and quenched samples supports this interpretation.

The existence of an ordered phase of the M_7O_{12}-type in this system has been postulated by Thornber *et al.* [3] and some structural parameters were later determined [4, 5]. However, the extent and stability of $Er_4Zr_3O_{12}$ there was not well defined. The present experiments show that the formation of $Er_4Zr_3O_{12}$ is a very sluggish process and, therefore, it can be assumed that some degree of cation ordering is present in its superstructure. The difference in ionic size between Zr^{4+} (0.079 nm) and Er^{3+} (0.089 nm) may favour cation ordering in $Er_4Zr_3O_{12}$ at low temperatures. It is known that the ordered vacancy phases of non-stoichiometric rare-earth oxides of the bigger cations, e.g., Ce, Pr and Tb [17–19], form rapidly due to high mobility in the anionic sub-lattice. In the present case, the sluggish formation of $Er_4Zr_3O_{12}$ cannot be fully explained using only high mobility in the oxygen sublattice. It seems evident that the ordering of the cations also plays an important role, which is in accord with the structural evidence found in the low-temperature form of $Yb_4Zr_3O_{12}$ [20].

The δ-structure appeared to be stable up to 1500° C, and above this temperature decomposed slowly (taking at least several weeks) into fluorite solid solution by an order–disorder process.

The constancy of the lattice parameters for $Er_4Zr_3O_{12}$ at both sides of its stoichiometric composition means that $Er_4Zr_3O_{12}$ is a line in the system. On the other hand, since the sequence of phase changes at 1500° C was: δ-phase (40 mol% Er_2O_3) → fluorite solid solution (45 mol% Er_2O_3) → two-phase (> 45 mol% Er_2O_3), a eutectoid reaction was considered to exist in this zone of the system. The above results, and also those obtained by Scott [21] on the ZrO_2–Y_2O_3 system, disagree with the results of Stubican *et al.* [22] who found that the δ-phase ($Y_4Zr_3O_{12}$) undergoes a peritectoid transformation into fluorite- and C-type solid solutions.

At higher erbia contents, two hexagonal phases of the $M_7O_{11.5}$ and M_7O_{11} types have also been found, and their composition, homogeneity ranges and thermal stabilities have been well established (see Fig. 8). In view of discrepancies found in the literature, no conclusive data can be given on these latter hexagonal phases.

Summarizing, a complex picture of phase transformations has been found in the present study for the ZrO_2–Er_2O_3 system. Although some additional work should be necessary to determine the exact location of the phase boundaries, the tentative diagram proposed here is in accord with the phase rule and also with the results obtained in the present experiments.

Acknowledgement

The author thanks Dr J. P. Coutures of the Laboratoire des Ultrarefractaires, Odeillo, France, for the facilities given for sample preparation in the solar furnace.

References

1. A. ROUANET, *Compt. Rend. Acad. Sci., Paris* **267c** (1968) 1581.
2. R. K. STEWART and O. HUNTER, Jr, *J. Amer. Ceram. Soc.* **53** (1970) 421.
3. M. R. THORNBER, D. J. M. BEVAN and E. SUMMERVILLE, *J. Sol. Stat. Chem.* **1** (1970) 545.
4. H. J. ROSSELL, *ibid.* **19** (1976) 103.
5. P. DURAN, *J. Amer. Ceram. Soc.* **62** (1977) 9.
6. R. RUH and H. J. GARRET, in "Thermal Analysis" edited by R. F. Schwinker and P. D. Garn (Academic Press, New York and London, 1969) p. 851.
7. K. K. SRIVASTAVA, R. N. PATIL, C. B. CHOUDHARY, K. V. G. K. GOKHALE and E. C. SUBBARAO, *Trans. J. Brit. Ceram. Soc.* **73** (1974) 85.
8. F. HUND, *Z. Phys. Chem.* **199** (1952) 142.
9. *Idem, Zeit. fur Electrochimie* **55** (1951) 363.
10. J. D. SCHIELTZ, J. W. PATTERSON and D. R. WILDER, *J. Electrochem. Soc.* **118** (1971) 1257.
11. S. F. BARTRAM, *Inorg. Chem.* **5** (1966) 749.
12. P. DURAN, C. PASCUAL and J. P. COUTURES, unpublished work, 1980.
13. F. M. SPIRIDINOV, V. A. STEPANOV, L. N. KOMISSAROVA and V. I. SPITSYN, *J. Less Common Met.* **14** (1968) 435.
14. M. PEREZ y JORBA, *Ann. Chim.* 7 (1962) 479.
15. F. M. SPIRIDINOV and L. N. KOMISSAROVA,

Zh. Neorg. Khim. **15** (1970) 875.
16. D. R. WILDER, J. D. BUCKLEY, D. W. STACY and J. K. JOHNSTONE, in "Study of Crystalline Transformations at Temperatures Above 2000 K" edited by Centre National de la Recherche Scientifique, Paris. No. 205 (1972) 335.
17. B. G. HYDE and L. EYRING, in "Rare Earth Research III" edited by L. Eyring (Gordon and Breach, New York, 1965).
18. B. G. HYDE, D. J. M. BEVAN and L. EYRING, *Phil. Trans. Roy. Soc.* **A259** (1966).
19. S. P. RAY, A. S. NOWICK and D. E. COX, *J. Sol. Stat. Chem.* **15** (1975) 344.
20. M. R. THORNBER and D. J. M. BEVAN, *ibid.* **1** (1970) 536.
21. H. G. SCOTT, *J. Mater. Sci.* **12** (1977) 311.
22. V. S. STUBICAN, R. C. HINK and S. P. RAY, *J. Amer. Ceram. Soc.* **61** (1978) 17.

Received 28 January and accepted 9 April 1981.